Article

Sequence-Specific, Self-Reporting Hairpin Inversion Probes

Kenneth A. Browne

J. Am. Chem. Soc., **2005**, 127 (6), 1989-1994• DOI: 10.1021/ja046369w • Publication Date (Web): 21 January 2005

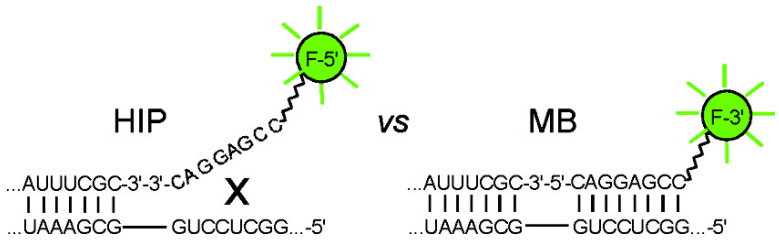

More About This Article

Additional resources and features associated with this article are available within the HTML version:

- Supporting Information
- Links to the 1 articles that cite this article, as of the time of this article download
- Access to high resolution figures
- Links to articles and content related to this article
- Copyright permission to reproduce figures and/or text from this article

View the Full Text HTML

J|A|C|S
ARTICLES
Published on Web 01/21/2005

Sequence-Specific, Self-Reporting Hairpin Inversion Probes

Kenneth A. Browne*

Contribution from Gen-Probe Incorporated, 10210 Genetic Center Drive, San Diego, California 92121

Received June 19, 2004; E-mail: kenb@gen-probe.com

Abstract: Sequence-specific probes for detecting target nucleic acids are the cornerstone of the genomics revolution (e.g., microarrays) and of molecular diagnostics. Molecular beacons are self-reporting, nucleic acid probes whose structure includes complementary terminal arm sequences and a loop that is complementary to a target sequence; fluorescence detection is by changes in proximity of fluorophore and quencher pairs attached on opposite arms. However, molecular beacon design is not as simple as attaching arbitrary arm sequences onto previously designed linear probes. The stem arms can also interact with flanking target sequences, changing the hybridization specificity; constantly adapting the arms to avoid such interactions, if not desired, increases design complexity. Herein, I report the use of inversion linkages in probe backbones leading to stem arms of sequence polarity opposite to that of the target-binding region, thereby eliminating potential hybridization of the arms with the target. Using two microbial sequence categories, thermal denaturation and target titration analyses demonstrate that these new hairpin inversion probes retain closed-state stability comparable to that of molecular beacons, contain easily designed arm sequences that do not interact with targets, and, therefore, can be used universally with optimized linear probe sequences.

Introduction

Due to the elegance of Watson−Crick interactions between complementary DNA and RNA sequences,[1] design of linear nucleic acid probes used to detect nucleic acid targets for genomic[2] and disease diagnostic[3] purposes is typically straightforward. Probe regions to sequences of interest are compared to other known sequences, unique regions chosen, and a probe region selected to optimize hybrid stability and specificity and to minimize influences from target secondary structure. Self-reporting nucleic acid probes, such as molecular beacons[4] (MBs), are well suited for homogeneous detection of target sequences; physical separation of hybridized and unhybridized probes is unnecessary since little fluorescent signal is yielded in the closed hairpin conformation due to proximal fluorophore and quencher moieties attached on or near opposite termini. Fluorescence increases upon hybridization of the loop region to a substantially complementary target since the increased rigidity of the double-stranded nucleic acid drives the stem arms and, hence, the fluorophore and the quencher apart (Scheme 1A).

Target nucleic acids from organisms of interest (e.g., viruses, bacteria) in, for example, environmental water samples can be detected with nanomolar concentrations of MBs. Populations of organisms may be sufficient for detection either prior to or after growing in culture. Alternatively, coupled with a target amplification technology, such as the PCR, the presence of scarce nucleic acids can be efficiently measured in real-time as

Scheme 1. Comparison of Structures and Modes of Interactions[a] between Target Nucleic Acids and (A) Molecular Beacons or (B) Hairpin Inversion Probes

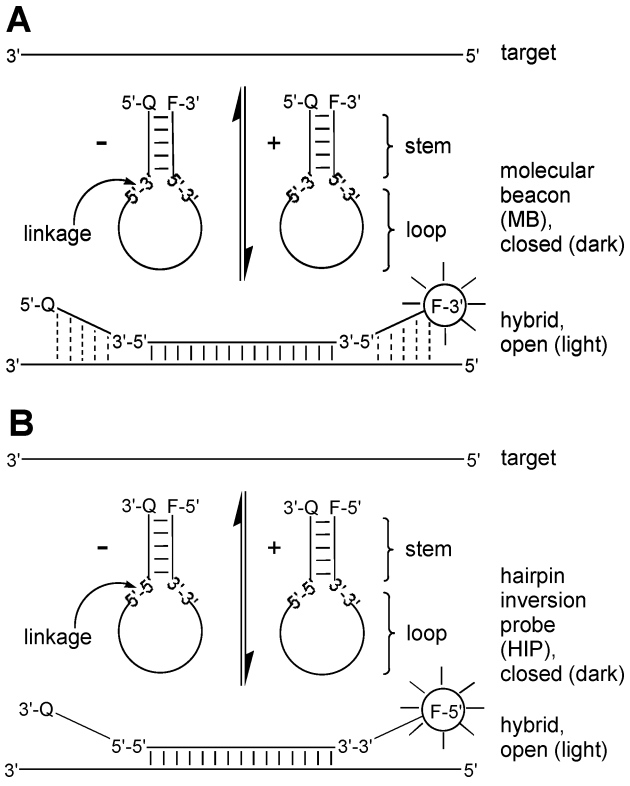

[a] Solid lines between nucleic acid strands indicate base pairing, while dashed lines indicate possible additional base pairing.

(1) Watson, J. D.; Crick, F. H. C. *Nature* **1953**, *171*, 737−738.
(2) Mir, K. U.; Southern, E. M. *Nat. Biotechnol*. **1999**, *17*, 788−792.
(3) Nelson, N. C.; Cheikh, A. B.; Matsuda, E.; Becker, M. M. *Biochemistry* **1996**, *35*, 8429−8438.
(4) Tyagi, S.; Kramer, F. R. *Nat. Biotechnol*. **1996**, *14*, 303−308.

10.1021/ja046369w CCC: $30.25

amplification reactions proceed,[4] eliminating the need for post-amplification detection and quantitation schemes. Thus, MBs are advantageous for a variety of high-throughput, homogeneous fluorescent detection systems.

For a given stem sequence, MB fluorescence and signal-to-noise ratios (*S*/*N*) were observed to vary with the same concentrations of targets from different species or with the nucleotide position in a single species target region. Unlike linear probes, which are typically designed to specifically hybridize along their length, hairpin probes can interact with a target sequence along the loop length *and* throughout part or all of the stem regions, effectively increasing the length of the probe. In fact, shared-stem MBs, dual-function stem MBs, and molecular torches have been designed to specifically take advantage of this effect. The target binding loop region and one arm of an otherwise apparently conventional MB hybridize to a target in shared-stem MBs;[5] this leads to higher affinity for target than for MBs but lower discrimination between closely related targets. Dual-function stem MBs[6] are similar to shared-stem MBs, except only part of the stem need be complementary to the flanking target sequence. Molecular torches[7] differ markedly from MBs in that one of the stem arms is designed to be largely complementary to a target sequence, while little if any of the loop region is designed to hybridize to the target; the long stem arms ensure a stable molecular torch self hybrid in the absence of target, maintaining proximity of terminal interacting labels.

A new type of self-reporting molecule, a hairpin inversion probe (HIP; Scheme 1B), has been designed. Like MBs, HIPs comprise a linear array of nucleotides that can form a hairpin structure, but unlike MBs, HIPs include inversion linkages that change the orientation of the nucleotide chain. By positioning these inversion linkages at the junctions between the stem arms and the loop, the arms have a linear orientation opposite to that of the loop (e.g., 3′→5′ stem arm and 5′→3′ loop sequences). Thus, the resultant stem region can form an antiparallel hybrid as found with other hairpin probes, but the stem and loop regions of the HIP are effectively disjunct from each other. Since mixed sequences strongly favor antiparallel hybridization,[8] upon addition of target polynucleic acids, a HIP can only hybridize to a target in its loop region while the stem arms are substantially precluded from interacting with flanking target sequences. Furthermore, by introducing discontinuity into the array of nucleic acids at these junctions, the loop sequence is less able to influence the stability of the stem sequence. To demonstrate the utility of these new hairpin inversion probes, HIPs were designed and synthesized, and their biophysical characteristics were compared to analogous MBs for hybridization to and detection of two series of microbial ribosomal RNA (rRNA) target sequences.

Materials and Methods

Synthesis. Oligonucleotides were synthesized in-house using solid-phase phosphite triester chemistry on ABI Expedite model 8909 automated synthesizers (Foster City, CA). Ribose and 2′-*O*-methyl ribose 3′-*β*-cyanoethyl (3′-CE) phosphoramidites were obtained from Pierce Biotechnology (Rockford, IL); deoxyribose 3′-CE phosphoramidites were from Proligo (Boulder, CO), and deoxyribose 5′-*β*-cyanoethyl (5′-CE) phosphoramidites were from Glen Research Corp. (Sterling, VA); other chemicals were from standard sources. The probes were either synthesized on dabcyl-linked controlled pore glass (CPG; Glen Research) and terminated with a 5′-fluorescein-labeled phosphoramidite or synthesized on fluorescein-linked CPG and terminated with a dabcyl-labeled phosphoramidite. Synthetic RNA target oligonucleotides were synthesized with ribose 5′-CE phosphoramidites, cleaved from the support, purified by polyacrylamide gel electrophoresis, and desalted with Waters Corp. Sep-Pak cartridges (Milford, MA), and subsequent ethanol-induced precipitation. After cleaving from the support, hairpin probe oligonucleotides were serially purified by polyacrylamide gel electrophoresis and reversed-phase HPLC (Beckman System Gold Nouveau (Fullerton, CA): Phenomenex 300 mm × 3.9 mm, 10 μm C18 column (Torrance, CA), linear gradient of 5−30% acetonitrile with H_2O containing 0.1 M triethylammonium acetate at 0.5 mL min^{-1} over 50 min) followed by desalting through Amersham Biosciences NAP-10 Sephadex G-25 columns (Piscataway, NJ).

To prepare oligonucleotides containing inversion internucleotide linkages, synthesis was first performed in the 5′→3′ direction with deoxyribose 5′-CE phosphoramidites until the first of the bidirectional segments was complete. The direction of synthesis was reversed to 3′→5′ by replacing the 5′-CE phosphoramidites with 2′-*O*-methyl ribose or deoxyribose 3′-CE phosphoramidites until the second of the bidirectional segments was complete; the junction between these two segments is a 3′−3′ linkage. The direction of synthesis was switched back to 5′→3′ by replacing the 3′-CE phosphoramidites with deoxyribose 5′-CE phosphoramidites until the third of the bidirectional segments was complete; the junction between these two segments is a 5′−5′ linkage.

Biophysical Characterizations. Thermal denaturation experiments were conducted in a Beckman DU-640 UV−vis spectrophotometer fitted with a Peltier temperature-controlled array for six 300 μL cuvettes (Fullerton, CA). Solutions consisting of 2 μM probe and 0 or 1 μM target were mixed with hybridization buffer (50 mM Tris/HCl, pH 8.0, 0.1 mM EDTA, 50 mM LiCl, 0.1% lithium dodecyl sulfate) and added to quartz cuvettes after zeroing and matching the cuvettes in Millipore (Bedford, MA) 18 MΩ deionized H_2O at 260 nm. Nucleic acids were annealed at 0.5 °C min^{-1} from 100 to 20 °C, then denatured at 0.5 °C min^{-1} from 20 to 100 °C. Changes in absorbance were recorded at 260 and 494 nm every 0.5 °C. Denaturation temperatures (T_ms) were calculated from the first derivatives of the different transitions.

Fluorescence characteristics of probes and probe/target hybrids were measured in a Labsystems Fluoroskan *Ascent* multi-well plate reader (Franklin, MA). After mixing 0.3 μM probe with 0−3 μM target in hybridization buffer in 96-well, flat bottomed, white Labsystems Cliniplates, the 100 μL solutions were covered with 75 μL silicone oil and incubated at 60 °C for 30 min, 42 °C for 30 min, and room temperature (ca. 23 °C) for 30 min. Each well was excited at 485 nm, and emissions were monitored at 530 nm at room temperature. Buffer-only fluorescence was subtracted from all measurements, and these buffer-corrected fluorescence and signal-to-noise ratios (*S*/*N*; eq 1) were plotted against target concentration.

$$\frac{S}{N} = \frac{\text{fluorescence}_{\text{open}} - \text{fluorescence}_{\text{buffer}}}{\text{fluorescence}_{\text{closed}} - \text{fluorescence}_{\text{buffer}}} \quad (1)$$

Apparent affinity constants (K_{app}) were calculated from parameters generated from the best fits of buffer-corrected fluorescence versus target concentration to the Sips model,[9] (eq 2):

$$F_{\text{target}} = F_{\max} \times \frac{(K_{\text{app}}c)^a}{(1 + K_{\text{app}}c)^a} \quad (2)$$

where F is fluorescence from the probe at a given target concentration or when the probe is completely open (max), c is the target concentra-

(5) Tsourkas, A.; Behlke, M. A.; Bao, G. *Nucleic Acids Res.* **2002**, *30*, 4208−4215.
(6) Bustamante, L. Y.; Crooke, A.; Martínez, J.; Díez, A.; Bautista, J. M. *BioTechniques* **2004**, *36*, 488−494.
(7) Becker, M. M.; Schroth, G. P. U.S. Patent 6,534,274, 2003.
(8) van de Sande, J. H.; Ramsing, N. B.; Germann, M. W.; Elhorst, W.; Kalisch, B. W.; Kitzing, E. v.; Pon, R. T.; Clegg, R. C.; Jovin, T. M. *Science* **1988**, *241*, 551−557.

Table 1. Nucleic Acid Sequence Alignments for Probes and Synthetic Targets

I.D.	Name[a,b,c]	Sequence[d,e,f,g,h]
PR10	*Eco*B1932(-) PR [2'-OMe]	5′- CGA CAA GGA AUU UCG C -3′
MB12	*Eco*B1932(-) MB2 [2'-OMe/DNA]	5′-D- GG CTC CTG CGA CAA GGA AUU UCG C CAG GAG CC-F-3′
HIP14	*Eco*B1932(-) HIP4 [2'-OMe/DNA]	3′-D- GG CTC CTG-5′-5′-CGA CAA GGA AUU UCG C-3′-3′-CAG GAG CC-F-5′
TAR15	*Eco*B1921–1958(+) [RNA]	3′- GC CUU GAA UGG GCU GUU CCU UAA AGC G AUG GAA UCC UG-5′
TAR19	*Eco*B1921–1958(+) comp9 [RNA]	3′- GC **CCC GAG GAC** GCU GUU CCU UAA AGC G **G**UG GAA UCC UG-5′
		| | |
		1950 1940 1930
	U. urealyticum, 1940–1977	3′- GC CUU **A**AA UGG GCU GUU CCU UAA AGC G AUG GAA UCC UG-5′
	M. hominis, 1928–1965	3′- G**U** C**A**U **A**AA U**C**G GCU GUU CCU UAA AGC G AUG GAA UCC UG-5′
PR80	*Cal*A1185(-) PR [DNA]	5′- GTC TGG ACC TGG TGA GTT TCC C -3′
MB82	*Cal*A1185(-) MB2 [DNA]	5′-D- GG CTC CTG GTC TGG ACC TGG TGA GTT TCC C CAG GAG CC-F-3′
HIP84	*Cal*A1185(-) HIP4 [DNA]	3′-D- GG CTC CTG-5′-5′-GTC TGG ACC TGG TGA GTT TCC C-3′-3′-CAG GAG CC-F-5′
TAR75	*Cal*A1174–1217(+) [RNA]	3′- UA GGA AUA ACA CAG ACC UGG ACC ACU CAA AGG G GCA CAA CUC AG-5′
TAR79	*Cal*A1174–1217(+) comp9 [RNA]	3′- UA **CCC GAG GAC** CAG ACC UGG ACC ACU CAA AGG G G**U**A CAA CUC AG-5′
		| | | |
		1210 1200 1190 1180
	B. dermatitidis, 1187–1230	3′- UA GGA AUA A**A**A CAG ACC UGG ACC ACU CAA AGG G GCA CAA CUC AG-5′
	C. neoformans, 1179–1222	3′- UA GGA **GUG** AU**A** CAG ACC UGG ACC ACU CAA AGG G GCA CAA CUC AG-5′

[a] Ten-series sequences are pan-bacterial probes and targets to/from the *Escherichia coli* O157:H7 23S rRNA reference sequence (NCBI Accession No. AE005174). [b] Eighty- and 70-series sequences are pan-fungal probes and targets to/from the *Candida albicans* 18S rRNA reference sequence (NCBI Accession No. E15168). [c] Regions and sequence alignments corresponding to *Ureaplasma urealyticum* 23S rRNA (NCBI Accession No. AF272605), *Mycoplasma hominis* 23S rRNA (NCBI Accession No. AF443616), *Blastomyces dermatitidis* 18S rRNA (NCBI Accession No. M55624), and *Cryptococcus neoformans* 18S rRNA (NCBI Accession No. M55625); only the regions corresponding to the synthetic targets are shown. [d] "F" denotes the attached fluorophore fluorescein, and "D" indicates the fluorescence quenching moiety dabcyl. [e] The "5′−5′" and "3′−3′" represent inverted internucleotidal linkages. [f] Underlined sequences are composed of deoxyribonucleotides; remaining probe sequences are composed of 2′-*O*-methyl ribonucleotides. [g] Deviations from the reference target sequences are indicated in bold. [h] Numbering to reference targets indicated underneath each class of reference sequences.

tion, and the exponent, a, is a parameter describing the affinity distribution.[10] The Sips model is an adaptation of the Langmuir isotherm for evaluating the affinity of molecules adsorbed to a surface. It has been used to measure equilibrium association−dissociation constants of analytes to/from surface-immobilized antibodies[10,11] and of target nucleic acids to surface-immobilized capture oligonucleotides.[9] The Sips isotherm was previously used to evaluate antibodies binding haptens in solution,[12] providing a final connection between using the Sips model for calculating affinities of analytes or targets to surface-immobilized antibodies or oligonucleotides and using this model for calculating the association constants between target nucleic acids and probes in solution. Hybridization and fluorescence measurements with rRNA targets were conducted in the same manner as with synthetic targets, except 40 nM probe and 0−50 ng/μL rRNA isolates were used.

Results and Discussion

Design. Bacterial and fungal model targets and probes to these targets (Table 1) were synthesized on an automated synthesizer using phosphoramidite monomers. The arms of the probes shared a common deoxyribonucleotide backbone, while the 2′-*O*-methyl ribonucleotide or deoxyribonucleotide backbone loop regions of the probes used for detection of pan-bacterial and pan-fungal species, respectively, were based on earlier optimized probe matrix designs.[13,14] Fluorescein was attached to the terminus of each probe (relative to the 3′ end of the loop regions), while dabcyl was attached to the opposite terminus. As shown in Scheme 1, the fluorophore and quencher of the HIP are necessarily on the stem arm termini opposite to that of the MB. In an alternate embodiment, the fluorophore and quencher may be on comparable termini on a HIP and a MB, but the fluorophore and quencher will then be in different orientations relative to the target-binding sequence of the HIP and the MB. GC clamps were used to maximize the stability of the stem regions, and the fluorophore was attached to a cytosine to substantially reduce nucleobase quenching that occurs from attachment to an adjacent guanine.[15] The different RNA target oligonucleotides included a reference sequence and a sequence linearly complementary over the length of the target-binding

(9) Peterson, A. W.; Wolf, L. K.; Georgiadis, R. M. *J. Am. Chem. Soc*. **2002**, *124*, 14601−14607.
(10) Vijayendran, R. A.; Leckband, D. E. *Anal. Chem*. **2001**, *73*, 471−480.
(11) Rabbany, S. Y.; Piervincenzi, R.; Judd, L.; Kusterbeck, A. W.; Bredehorst, R.; Hakansson, K.; Ligler, F. S. *Anal. Chem*. **1997**, *69*, 175−182.
(12) Karush, F.; Karush, S. S. In *Methods in Immunology and Immunochemistry*; Williams, C. A., Chase, M. W., Eds.; Academic Press: New York, 1971; Vol. 3, pp 383−393.
(13) Hogan, J. J. U.S. Patent 5,840,488, 1998.
(14) Marlowe, E. M.; Hogan, J. J.; Hindler, J. F.; Andruszkiewicz, I.; Gordon, P.; Bruckner, D. A. *J. Clin. Microbiol*. **2003**, *41*, 5127−5133.
(15) Marras, S. A.; Kramer, F. R.; Tyagi, S. *Nucleic Acids Res*. **2002**, *30*, e122.

region plus 10 additional contiguous nucleotides from the stem arms. To take advantage of more realistic affinity between probes and targets due to flanking sequences, the synthetic targets were three nucleotides longer on each terminus than their respective probes.[16]

For a given sequence, the following hypotheses were generated from the description of HIP design. First, the stability of a HIP stem hybrid will be comparable to that from a MB if the arm lengths, sequences, and orientations (antiparallel) are the same and the loop size and sequence are the same [1]. Second, the affinity of the MB for the target will increase, while the affinity of the HIP for the target will not change when target sequences flanking the loop contain increasing numbers of nucleobases that are complementary to those in the arm sequences [2]. Analytical methods were chosen to test these hypotheses. Denaturation temperatures (T_ms) provide straightforward values of the affinity of stem arms for each other and of probes for targets, but they do not provide information on changes in fluorescence, the typical method of monitoring probes such as MBs. Fluorescence spectroscopy is very sensitive and can measure subtle changes in the relationship between the fluorophore and the quenching moieties (e.g., separation due to target-induced opening), but the fluorophore and the quencher are also sensitive to their local environments relative to their attachment positions and orientations on oligonucleotides. The following results must be considered with the above hypotheses and caveats in mind.

Affinity of Probes for Target Sequences. Changes in affinity between a probe's arms and between probe:target hybrids were measured by UV−vis spectroscopy as a function of temperature (Table 2). T_ms calculated from changes at 260 nm were due to nucleobase absorbance, and those calculated from changes at 494 nm were due to fluorescein absorbance. The T_ms determined at the different wavelengths for MBs or HIPs to a given target sequence were typically within ca. 0.5−1.5 °C of each other. From this point and the consistent stem T_m values observed at 494 nm even in the presence of target, it is clear that changes at 494 nm are primarily indicative of the separation of fluorescein from dabcyl upon hairpin denaturation. Furthermore, in terms of assay performance, the T_m of the HIP stem for a given sequence was not detrimentally lower (ca. 4−7 °C) than the T_m for the related MB stem, consistent with hypothesis [1]. The decrease observed in T_m was likely due to differences in contiguous base stacking at the 3′−5′ stem-loop junctions of the MBs from those at the 5′−5′ (lengthened linkages) and 3′−3′ (shortened linkages) junctions of the HIPs. The T_ms of the pan-fungal probe stems were ca. 3−4 °C lower than those of the pan-bacterial probes, consistent with the larger loop size (increased entropy) of the pan-fungal probes.

Changes in absorbance at 260 nm could arise from hairpin denaturation, probe:target hybrid denaturation, or both. These possibilities can be largely distinguished by comparison of the T_ms at 260 and 494 nm. For example, the pan-bacterial MB12:TAR19 hybrid had a thermal transition at 69 °C at 260 nm and 67 °C at 494 nm, indicating the T_m of the MB stem was in this range (Table 2). A second thermal transition observed at 260 nm occurred at 81 °C, corresponding to denaturation of the MB from the target. Some thermally induced absorbance transitions may be obscured by other transitions. Only one T_m was observed for the MB12:TAR15 hybrid at 260 nm; the absorbance changes corresponding to the thermal transitions for the MB:target hybrid and the MB stem were shown to substantially overlap and, hence, the T_m for the MB:target was estimated to also be ca. 68 °C, consistent with the T_m of the linear probe for the reference target (PR10:TAR15). While the extended hybrid formed between MB12 and TAR19 had a higher T_m than the same MB with the reference target, the T_m of HIP14 with the same targets was essentially the same for each hybrid (ca. 63−65 °C) and not substantially different from that of the HIP stem (ca. 62 °C), indicating little interaction between the stem arms and the flanking target sequences. The thermal transitions at 260 nm for the pan-fungal probe:target hybrids also demonstrated the same trends. (i) The T_m of the MB:extended complementary target was greater than that of the MB:reference target; and (ii) the T_m of the HIP:extended complementary target was about the same as that of the HIP:reference target. These results support hypothesis [2].

Table 2. Summary of Probe and Probe:Target Affinity Interaction Characteristics with Synthetic Targets

nucleic acid I.D.[a]	T_m @ 260 nm (°C)[b]		T_m @ 494 nm (°C)[b]	S/N[c]	K_{app} (M^{-1})[c]
Pan-Bacterial					
PR10:TAR15		68.5			
MB12	68.3		67.7		
MB12:TAR15	67.3	nd[d]	68.7	50	1.1×10^6
MB12:TAR19	68.6	81.1	67.3	138	9.2×10^6
HIP14	58.8		60.3		
HIP14:TAR15	nd	63.2	61.7	40	5.8×10^6
HIP14:TAR19	nd	65.3	61.8	46	4.9×10^6
Pan-Fungal					
PR80:TAR75		69.7			
MB82	62.7		63.3		
MB82:TAR75	nd	71.2	64.7	23	6.9×10^6
MB82:TAR79	65.3	80.7	64.2	35	7.5×10^6
HIP84	nd		59.3		
HIP84:TAR75	nd	67.2	56.2	29	6.2×10^6
HIP84:TAR79	58.2	68.3	57.8	31	7.0×10^6

[a] See Table 1 for sequences and accession numbers. [b] T_m determined from the first derivative of absorbance versus temperature plots. [c] Signal-to-noise ratios at 10:1 target:probe and apparent association constants determined from eqs 1 and 2, respectively, when applied to fluorescence data, such as those in Figure 1. [d] Not detected.

Fluorescence Responses from Probes Hybridizing to Target Sequences. Increasing concentrations of synthetic targets were allowed to anneal with a constant amount of probe. As seen in Figure 1A,B, fluorescence increased as a function of target concentration until reaching a plateau at high target concentration. The fluorescence for the HIPs was higher than that for comparable MBs, likely due to the different environments in which fluorescein and dabcyl exist with respect to their attachment on the probes. The *S*/*N* increased for MBs with increasing complementarity to the target (Figure 1C,D, Table 2); in fact, for the pan-bacterial MB, the *S*/*N* was more than 150% greater when this probe hybridized to the target with extended complementarity than to the reference target. These substantial differences in *S*/*N* were due to the increased affinity with the extended target and/or the change in physicochemical environment for the fluorescein and/or dabcyl with the target containing extended complementarity. A lesser difference seen for pan-fungal MB82 was likely due to its already long target binding region. The *S*/*N* values for the HIP hybrids with the

(16) Burkard, M. E.; Kierzek, R.; Turner, D. H. *J. Mol. Biol.* **1999**, *290*, 967−982.

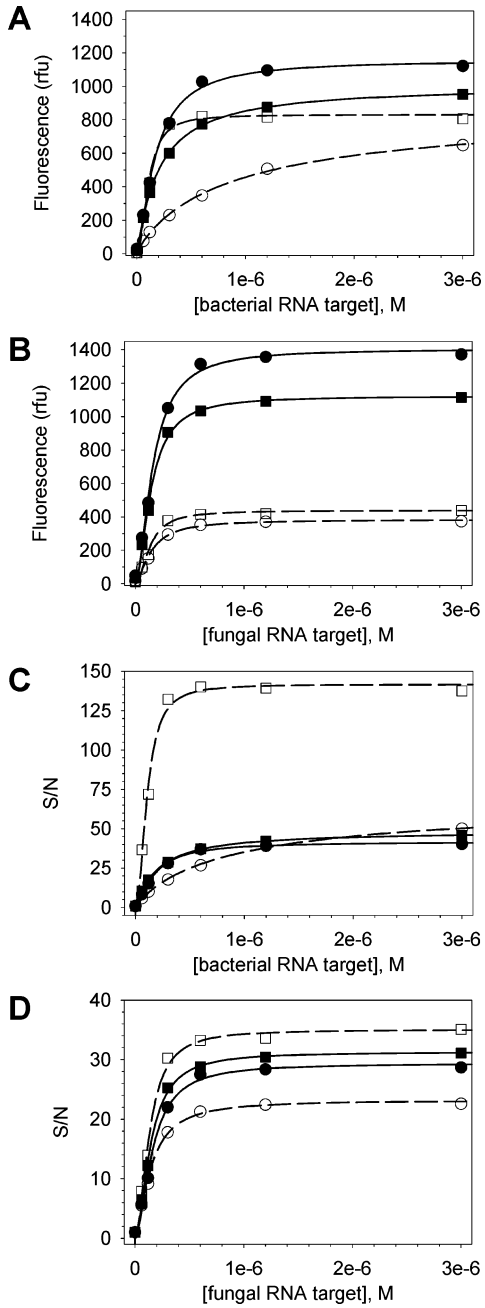

Figure 1. Background-subtracted fluorescence (A and B) or *S*/*N* (C and D) versus synthetic target concentration at a constant probe concentration (0.3 μM) for (A and C) pan-bacterial probes and (B and D) pan-fungal probes. MB with reference target (○) and with extended complementary target (□); HIP with reference target (●) and with extended complementary target (■). Curves through data points are best fits to the Sips model.

targets containing extended complementarity were similar to those with the reference targets. The data from the plots in Figure 1 were next fitted to the Sips model (eq 2), yielding apparent affinity constants (K_{app}) for the probes to the targets. On a probe-by-probe basis, K_{app} roughly followed the same pattern as *S*/*N* and T_m of the probe:target hybrids (Table 2), further supporting hypothesis [2].

To be practical for nucleic acid sequence detection applications, HIPs need to be sensitive, specific, and preferably quantitative. To test sensitivity and specificity, each hairpin probe was allowed to hybridize with increasing concentrations of rRNA from three bacterial and three fungal species. If

Table 3. Summary of Probe:Target Interaction Characteristics with Microbial rRNA

probe[a]	rRNA target[a]	limit of detection (ng/μL rRNA)[b]	quantitation curve (*S*/*N* per ng/μL rRNA)[c]
MB12	*E. coli*	25	0.019
MB12	*U. urealyticum*	25	0.016
MB12	*M. hominis*	25	0.026
MB12	*C. albicans*	nd[d]	0
MB12	*B. dermatitidis*	nd	0
MB12	*C. neoformans*	nd	0
HIP14	*E. coli*	2.5	0.098
HIP14	*U. urealyticum*	5.0	0.10
HIP14	*M. hominis*	2.5	0.14
HIP14	*C. albicans*	nd	0
HIP14	*B. dermatitidis*	nd	0
HIP14	*C. neoformans*	nd	0
MB82	*E. coli*	nd	0
MB82	*U. urealyticum*	nd	0
MB82	*M. hominis*	nd	0
MB82	*C. albicans*	2.5	0.45
MB82	*B. dermatitidis*	2.5	0.55
MB82	*C. neoformans*	2.5	0.58
HIP84	*E. coli*	nd	0
HIP84	*U. urealyticum*	nd	0
HIP84	*M. hominis*	nd	0
HIP84	*C. albicans*	2.5	0.19
HIP84	*B. dermatitidis*	1.0	0.23
HIP84	*C. neoformans*	1.0	0.22

[a] See Table 1 for sequences and accession numbers. [b] Limit of detection (LOD) defined from the 99% confidence interval as 3σ above the noise level; the next greater target concentrations that were actually measured are shown as LOD. [c] Quantitation curve slope (*S*/*N* = slope × rRNA concentration) in the linear range ($R^2 > 0.95$ for each) from the limit of detection to 50 ng/μL (33.2 nM *E. coli*) rRNA in the presence of 40 nM probe. [d] Not detected.

specific, the bacterial probes should detect all of the bacterial species' rRNA and none of the fungal rRNA, while the fungal probes should detect all of the fungal species' rRNA and none of the bacterial rRNA. The different rRNAs have different mismatch patterns in the 3′ target regions opposite the stem arms than the reference sequences (*Escherichia coli* and *Candida albicans*; Table 1); *Ureaplasma urealyticum* has one additional mismatch (dC:G → dC:A); *Mycoplasma hominis* has three matched or wobble base pairs exchanged for three mismatches (dT:G → dT:C, dC:G → dC:A, dG:U → dG:A); *Blastomyces dermatitidis* has one additional matched base pair (dT:C → dT:A), and *Cryptococcus neoformans* exchanges one mismatch for another and two mismatches for two matches (dT:C → dT:U, dC:A → dC:G, dC:A → dC:G). After measuring fluorescence, *S*/*N* ratios were calculated from eq 1 at each of the added rRNA concentrations. MB12 detected a minimum of 25 ng/μL of each of the bacterial rRNAs, while HIP14 detected a minimum of 2.5−5 ng/μL of each of the bacterial species (Table 3); neither bacterial probe detected any of the fungal species (*S*/*N* ∼ 1 at all rRNA concentrations). Analogous results were found with the pan-fungal probes; bacterial rRNA did not increase fluorescence above background, while 2.5 ng/μL of fungal rRNA was detected by MB82 and 1−2.5 ng/μL of the fungal species rRNA was sufficient for detection by HIP84. Thus, all of the hairpin probes are specific and sensitive down to at least 25ng/μL rRNA, depending on species/sequence being detected.

The fluorescence and *S*/*N* of the hairpin probes increased linearly with increasing concentrations of rRNA from different microbial species and were quantitative from the limit of

detection through at least the maximum rRNA concentration tested (50 ng/μL). As is evident from Table 3, the slopes of these curves, *S*/*N* per ng/μL rRNA, vary depending on probe type and target. *S*/*N* per ng/μL rRNA is a measure of the increase in detection of an analyte signal above the noise level, relative to known concentrations of analyte.[17] While fluorescence units are relative, the *S*/*N* is a dimensionless form of the observable that takes into account signal from both the open and closed forms of the hairpin probes and can be used to compare results across fluorescence detector platforms or other detection platforms. Thus, given a *S*/*N* in one detection system for a probe and analyte pair, calculating the quotient with the *S*/*N* per ng/μL slope will yield the target concentration at that level of detection. The magnitudes of the slopes depend on multiple factors that are beyond the presented limited data set and the scope of this proof of concept, but the factors likely include changes in the sequences opposite the hairpin stem arms and longer-range secondary structure of the rRNA targets, both of which can affect affinity of a probe to a complementary sequence. Variation in the quantitation curves and LOD among target species is consistent with the up to 3-fold differences in percent hybridization observed for the linear probes complementary to rRNA from different target species.[13] That the slopes are linear and greater than zero for the bacterial probes with each bacterial target and for the fungal probes with each fungal target, while the slopes for bacterial probes with fungal targets and for fungal probes with bacterial targets were zero, demonstrates that each probe quantitatively detects the specific targets as designed. It can therefore be seen that the HIPs, like MBs, are both specific and quantitative.

(17) Lowe, M.; Spiro, A.; Zhang, Y.-Z.; Getts, R. *Cytometry* **2004**, *60A*, 135−144.

Thus, the new HIPs have been compared to the well-known MBs in structural design and performance in homogeneous detection of microbial nucleic acid sequences. The stem arms of MBs hybridize to varying degrees with target sequences, while the arms that make up the stem of HIPs do not interact with the sequences flanking the probe-binding region due to their inverted sugar−phosphate linkage orientations. This novel configuration maintains the target affinity and specificity of detection found with linear probes without substantial changes in sensitivity relative to MB designs. Furthermore, eliminating the need for adjustment of the arm sequences for different target sequences by uncoupling the target binding and the arm sequences is a substantial step toward a "universal" stem sequence for hairpin, self-reporting fluorescence probes that yield high *S*/*N* and that can be used in a cassette fashion on different linear probe designs.

Acknowledgment. M. Majlessi and the Oligonucleotide Synthesis Group at Gen-Probe have my sincere thanks for their excellent syntheses of the complex oligonucleotide constructs presented in this article, as does P. Gordon for generously providing ribosomal RNA isolates.

Note Added in Proof

A patent application has been published proposing polynucleotide stem-loop structures designed so that the polynucleotides that form the stems are in the reverse orientation with respect to that of the loop region (Shchepinov, M. S.; Southern, E. M. U.S. Patent Appl. 10/479,887, 2004).

JA046369W